

CENTRAL EXCLUSIVE PRODUCTION AT THE LHCb*

MURILO SANTANA RANGEL

on behalf of the LHCb Collaboration

UFRJ — Federal University of Rio de Janeiro, Brasil

(Received March 6, 2019)

Central exclusive production studies at the LHCb are reported. A search is performed for the central exclusive production of pairs of charmonia produced in proton–proton collisions using data corresponding to an integrated luminosity of 3 fb^{-1} collected at centre-of-mass energies of 7 and 8 TeV. Pairs of $J/\psi J/\psi$ and $J/\psi \psi(2S)$ are observed which is a unique process at hadron machines in which particles are produced via colourless propagators. The central exclusive production of J/ψ and $\psi(2S)$ mesons is measured in pp collisions at a centre-of-mass energy of 13 TeV, and backgrounds are significantly reduced compared to previous measurements through the use of new forward shower counters.

DOI:10.5506/APhysPolBSupp.12.941

1. Introduction

Central exclusive production (CEP) [1] in pp collisions is a diffractive process in which the protons remain intact and a particle (system of particles) is produced through the fusion of photons and/or colourless strongly coupled objects, the so-called Pomerons. In some models, the cross section can be predicted in perturbative quantum chromodynamics (QCD) with a strong dependence on the gluon parton distribution function (PDF). Therefore, measurements of CEP provide tests of the interplay of the hard and soft regime of QCD.

The LHCb Collaboration has measured exclusive processes in pp and PbPb collisions at different centre-of-mass energies [2–7]. In this report, we present details of the observation of charmonium pairs produced exclusively at $\sqrt{s} = 7 \text{ TeV}$ and $\sqrt{s} = 8 \text{ TeV}$ [4], and the measurement of centrally exclusively produced J/ψ and $\psi(2S)$ at $\sqrt{s} = 13 \text{ TeV}$ [6].

* Presented at the Diffraction and Low- x 2018 Workshop, August 26–September 1, 2018, Reggio Calabria, Italy.

2. LHCb experiment

The LHCb detector [8, 9] is a single-arm forward spectrometer covering the pseudorapidity range of $2 < \eta < 5$, designed for the study of particles containing b or c quarks. The detector includes a high-precision tracking system consisting of a silicon-strip vertex detector (VELO) surrounding the pp -interaction region. Photons, electrons and hadrons are identified by a calorimeter system consisting of scintillating-pad (SPD) and preshower detectors, an electromagnetic calorimeter and a hadronic calorimeter. Muons are identified by a system composed of alternating layers of iron and multi-wire proportional chambers [10]. The trigger consists of a hardware stage, based on information from the calorimeter and muon systems, followed by a software stage, which applies a full event reconstruction.

In 2015, the addition of new forward shower counters (HeRSChE) [11] extended the pseudorapidity region in which particles can be vetoed. The forward shower counters consist of five planes of scintillators with three planes at 114, 19.7 and 7.5 m upstream of the interaction point, and two downstream at 20 and 114 m. At each location, there are four quadrants of scintillators, whose information is recorded in every beam crossing by photomultiplier tubes, giving a total of 20 channels in HeRSChE. These are calibrated using data taken without beams circulating at the end of each LHC fill. The pseudorapidity ranges covered by VELO and HeRSChE are different. For VELO, the region is $-3.5 < \eta < -1.5$ and $2 < \eta < 5$, and for HeRSChE, the region is $-10 < \eta < -5$ and $5 < \eta < 10$.

3. Central exclusive production of charmonium pairs

The central exclusive production of charmonium pairs is studied using a dataset corresponding to an integrated luminosity of $946 \pm 33 \text{ pb}^{-1}$ collected in 2011 at a centre-of-mass energy $\sqrt{s} = 7 \text{ TeV}$ and $1985 \pm 69 \text{ pb}^{-1}$ collected in 2012 at $\sqrt{s} = 8 \text{ TeV}$. The selected signature for exclusive charmonium pairs are events containing four muons, at most two photons, and no other activity.

The analysis is performed in the fiducial region where the dimeson system has a rapidity between 2.0 and 4.5. The invariant masses of oppositely charged muon candidates is shown in the left plot of Fig. 1. Requiring that one of the masses is within -200 MeV and $+65 \text{ MeV}$ of the known J/ψ or $\psi(2S)$ mass, the invariant mass of the other two tracks is shown in the right plot of Fig. 1.

Three background components are considered: non-resonant production, feed-down from the exclusive production of other mesons, and inelastic production of mesons where one or both protons dissociate. The non-resonant background is only considered for the $J/\psi J/\psi$ analysis and it is calculated

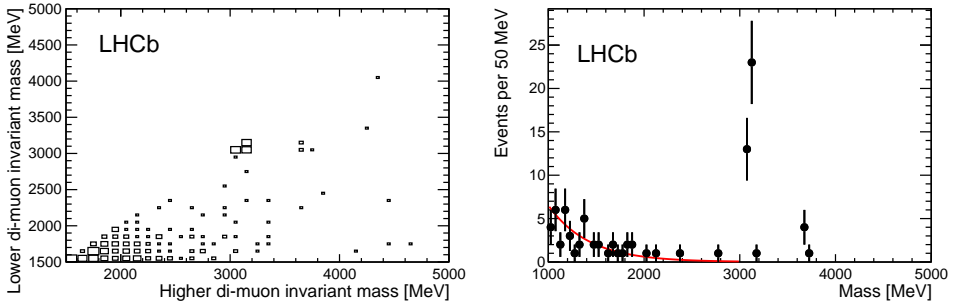


Fig. 1. Left: Invariant masses of pairs of oppositely charged muons in events with exactly four tracks. Right: Invariant mass of the second pair of tracks where the first pair has a mass consistent with the J/ψ or $\psi(2S)$ meson.

by fitting an exponential to the non-signal region in Fig. 1 and extrapolating under the signal. The feed-down background is estimated using simulated events normalised by control samples.

The cross sections are quoted for observed mesons to be exclusively produced considering the tracks and electromagnetic deposits found in the LHCb acceptance. Nonetheless, to compare with theoretical predictions that are usually quoted for the elastic process without proton break-up, an attempt is made to quantify the elastic fraction in the $J/\psi J/\psi$ sample, using the distribution of squared transverse momentum, p_T^2 , and describing the elastic and proton-dissociation components by different exponential functions.

Acceptance and efficiency corrections are applied and systematic uncertainties are estimated using simulation and data-driven methods. The cross sections, at an average energy of 7.6 TeV, for the dimeson system to be in the rapidity range of $2.0 < y < 4.5$ with no other charged or neutral energy inside the LHCb acceptance are measured to be

$$\begin{aligned}
 \sigma^{J/\psi J/\psi} &= 58 \pm 10(\text{stat.}) \pm 6(\text{syst.}) \text{ pb}, \\
 \sigma^{J/\psi \psi(2S)} &= 63_{-18}^{+27}(\text{stat.}) \pm 10(\text{syst.}) \text{ pb}, \\
 \sigma^{\psi(2S) \psi(2S)} &< 237 \text{ pb}, \\
 \sigma^{\chi_{c0} \chi_{c0}} &< 69 \text{ nb}, \\
 \sigma^{\chi_{c1} \chi_{c1}} &< 45 \text{ pb}, \\
 \sigma^{\chi_{c2} \chi_{c2}} &< 141 \text{ pb},
 \end{aligned}$$

where the upper limits are at 90% C.L.

4. Central exclusive production of J/ψ and $\psi(2S)$ mesons

The central exclusive production of J/ψ and $\psi(2S)$ is studied using a dataset corresponding to an integrated luminosity of $204 \pm 8 \text{ pb}^{-1}$ in pp collisions at $\sqrt{s} = 13 \text{ TeV}$ used in this analysis. Exclusive J/ψ and $\psi(2S)$ candidates are selected through their characteristic signature at a hadron collider: a pp interaction devoid of any activity saves the charmonium that is reconstructed from its decay to two muons.

Two reconstructed muons are required in the region of $2.0 < \eta < 4.5$, with an invariant mass within $\pm 65 \text{ MeV}$ of the known J/ψ or $\psi(2S)$ mass [12] and p_{T}^2 of the dimuon below 0.8 GeV^2 . Events with additional VELO tracks or photons with transverse energies above 200 MeV or with significant activity above noise in HeRSChEL are removed. The data in the nonresonance regions constitute an important calibration sample. The p_{T}^2 distribution of these dimuons with and without the requirement on HeRSChEL is shown in Fig. 2 and is significantly peaked towards low values due to the long-range electromagnetic interaction. The fraction of electromagnetic CEP events in this sample is determined from a fit to the p_{T}^2 distribution with two components: a signal shape taken from simulated events and an inelastic background modelled with the sum of two exponential functions.

Three background sources are considered: nonresonant dimuon production; feed-down of CEP $\chi_{cJ}(1P)$ or $\psi(2S)$ to J/ψ mesons and other undetected particles; and nonexclusive events where the proton dissociates but the remnants remain undetected. The amount of nonresonant background is determined from the fit shown in Fig. 2, where the signals are modelled with two Crystal Ball functions [13] and the nonresonant background with the sum of two exponential functions. The $\psi(2S)$ feed-down background in the

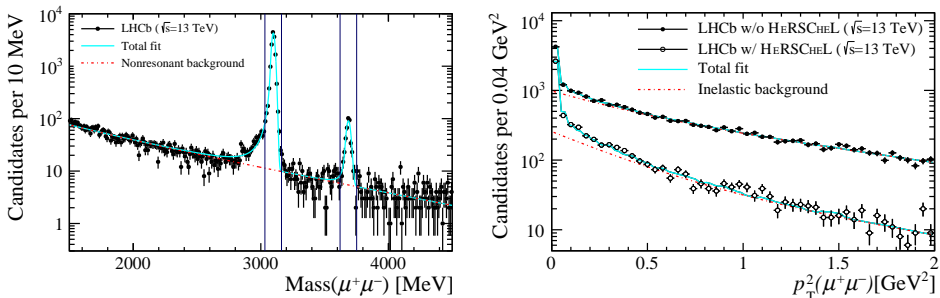


Fig. 2. Left: Invariant mass distribution of dimuon candidates. The J/ψ and $\psi(2S)$ mass windows of the signal regions are indicated by the vertical lines. Right: Transverse momentum squared for dimuons in the nonresonant region. The upper distributions are without any requirement on HeRSChEL: the lower are with the HeRSChEL veto applied.

J/ψ selection is determined using simulated events normalised to data control samples, while the $\chi_{cJ}(1P)$ feed-down background is determined using a data calibration sample which contains events without the zero photons requirement. The fraction of nonexclusive events due to proton dissociation is determined through the p_T^2 distribution of the J/ψ and the $\psi(2S)$ candidates, after a background subtraction to remove contributions coming from the electromagnetic nonresonant and feed-down backgrounds. The total feed-down ratio from $\psi(2S)$ and $\chi_{cJ}(1P)$ mesons is 0.060 ± 0.002 , to be compared to 0.101 ± 0.009 in the previous analysis [3], which means that the addition of HeRSChEL suppresses events with proton dissociation, which are more numerous in the double-Pomeron exchange process that mediates $\chi_{cJ}(1P)$ production.

The number of selected events is corrected by the effective luminosity, efficiencies and purity to calculate the differential cross sections shown in Fig. 3. Summing these differential results leads to measurements of the product of the cross sections and branching fractions, where both muons are within the fiducial region, $2.0 < \eta < 4.5$:

$$\begin{aligned} \sigma_{J/\psi \rightarrow \mu^+ \mu^-} (2 < \eta < 4.5) &= 435 \pm 18 \pm 17 \pm 16 \text{ pb}, \\ \sigma_{\psi(2S) \rightarrow \mu^+ \mu^-} (2 < \eta < 4.5) &= 11.1 \pm 1.1 \pm 0.3 \pm 0.4 \text{ pb}. \end{aligned}$$

The first uncertainties are statistical and include the uncertainties on the data-driven efficiencies and purities, the second are systematic, and the third are due to the luminosity determination.

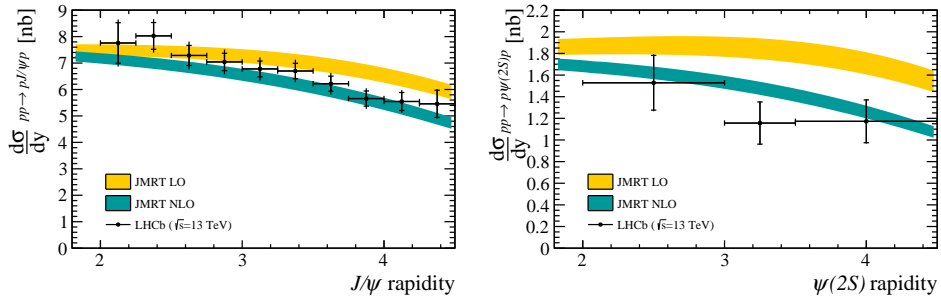


Fig. 3. Differential cross sections compared to LO and NLO theory JMRT predictions [14, 15] for the J/ψ meson (left) and the $\psi(2S)$ meson (right). The inner error bar represents the statistical uncertainty; the outer is the total uncertainty. Since the systematic uncertainty for the $\psi(2S)$ meson is negligible with respect to the statistical uncertainty, it is almost not visible in the right-hand side figure.

5. Conclusions

The production of pairs of $J/\psi J/\psi$ and $J/\psi\psi(2S)$ in the absence of other activity in the LHCb acceptance is observed and the measurements are in agreement with preliminary theoretical predictions. No signal is observed for the production of pairs of P-wave charmonia and upper limits on the cross sections are set. The cross sections for exclusive J/ψ and $\psi(2S)$ using scintillators in the forward region to reduce backgrounds are measured and compared to theory. The measurements are found to be in better agreement with NLO predictions.

REFERENCES

- [1] M.G. Albrow, T.D. Coughlin, J.R. Forshaw, *Prog. Part. Nucl. Phys.* **65**, 149 (2010) [arXiv:1006.1289 [hep-ph]].
- [2] LHCb Collaboration, LHCb-CONF-2011-022.
- [3] R. Aaij *et al.* [LHCb Collaboration], *J. Phys. G* **41**, 055002 (2014) [arXiv:1401.3288 [hep-ex]].
- [4] R. Aaij *et al.* [LHCb Collaboration], *J. Phys. G* **41**, 115002 (2014) [arXiv:1407.5973 [hep-ex]].
- [5] R. Aaij *et al.* [LHCb Collaboration], *J. High Energy Phys.* **1509**, 084 (2015) [arXiv:1505.08139 [hep-ex]].
- [6] R. Aaij *et al.* [LHCb Collaboration], *J. High Energy Phys.* **1810**, 167 (2018) [arXiv:1806.04079 [hep-ex]].
- [7] LHCb Collaboration, LHCb-CONF-2018-003.
- [8] A.A. Alves Jr. *et al.* [LHCb Collaboration], *JINST* **3**, S08005 (2008).
- [9] R. Aaij *et al.* [LHCb Collaboration], *Int. J. Mod. Phys. A* **30**, 1530022 (2015) [arXiv:1412.6352 [hep-ex]].
- [10] A.A. Alves Jr. *et al.*, *JINST* **8**, P02022 (2013) [arXiv:1211.1346 [physics.ins-det]].
- [11] K. Carvalho Akiba *et al.*, *JINST* **13**, P04017 (2018) [arXiv:1801.04281 [physics.ins-det]].
- [12] C. Patrignani *et al.* [Particle Data Group], *Chin. Phys. C* **40**, 100001 (2016) and 2017 update.
- [13] T. Skwarnicki, "A Study of the Radiative Cascade Transitions Between the Upsilon- prime and Upsilon Resonances, Ph.D. Thesis, Institute of Nuclear Physics, Kraków, 1986, DESY-F31-86-02.
- [14] S.P. Jones, A.D. Martin, M.G. Ryskin, T. Teubner, *J. High Energy Phys.* **1311**, 085 (2013) [arXiv:1307.7099 [hep-ph]].
- [15] S.P. Jones, A.D. Martin, M.G. Ryskin, T. Teubner, *J. Phys. G* **41**, 055009 (2014) [arXiv:1312.6795 [hep-ph]].